

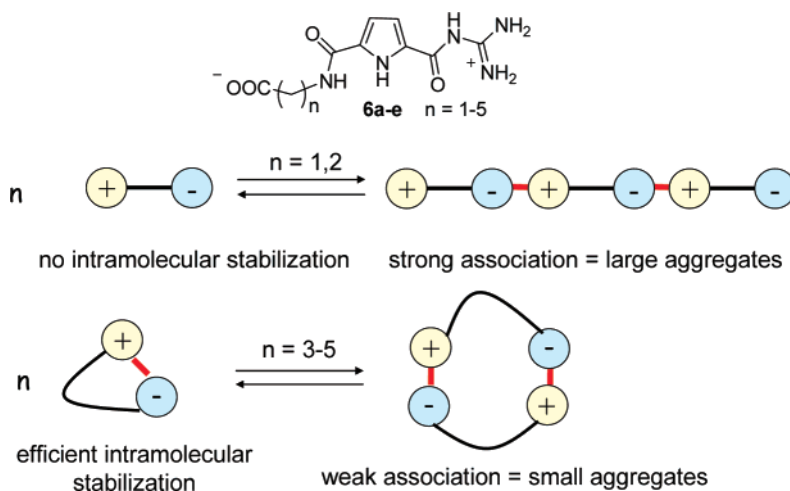
Synthesis and Self-Association Properties of Flexible Guanidiniocarbonylpyrrole–Carboxylate Zwitterions in DMSO: Intra- versus Intermolecular Ion Pairing

Carsten Schmuck,^{*,†} Thomas Rehm,[†] Lars Geiger,[†] and Mathias Schäfer[‡]

Universität Würzburg, Institut für Organische Chemie, Am Hubland, 97074 Würzburg, Germany, and
Universität zu Köln, Institut für Organische Chemie, Greinstrasse 4, 50939 Köln, Germany

schmuck@chemie.uni-wuerzburg.de

Received March 28, 2007



We have synthesized a new class of flexible zwitterions **6a–e**, in which a carboxylate is linked via an alkyl chain with variable length (one to five methylene groups) to a guanidiniocarbonylpyrrole cation. The self-association properties of these zwitterions were determined by NMR dilution studies in DMSO and by ESI-MS experiments. The stability and hence also the size of the aggregates formed via self-assembly is critically dependent on the length and therefore flexibility of the spacer. Whereas the smallest zwitterion **6a** forms large aggregates already at low concentrations, the more flexible zwitterions only form small oligomers (**6b**) or dimers (**6c–e**) at much larger concentrations. The differences between the five zwitterions can be explained based on the different extent of *intramolecular* ion pairing within the monomers. Any intramolecular ion pairing, which becomes possible with increasing linker length, stabilizes the monomer and therefore destabilizes any oligomer.

Introduction

In the field of supramolecular chemistry intense research is momentarily directed toward the design of new building blocks for supramolecular polymers, e.g., self-complementary molecules that because of efficient self-assembly in solution give rise to large aggregates.¹ The study of such building blocks might be useful for the design of supramolecular polymers that

function even in polar solutions (e.g., aqueous media).² So far the vast majority of self-assembling systems relies mainly on hydrogen bonds³ because of their directionality and specificity. The main drawback of hydrogen bonds is however their limited strength in polar solutions.⁴ Hence, under polar conditions

* Author to whom correspondence should be addressed. Fax: + 49 931 8884626.

[†] Universität Würzburg.

[‡] Universität zu Köln.

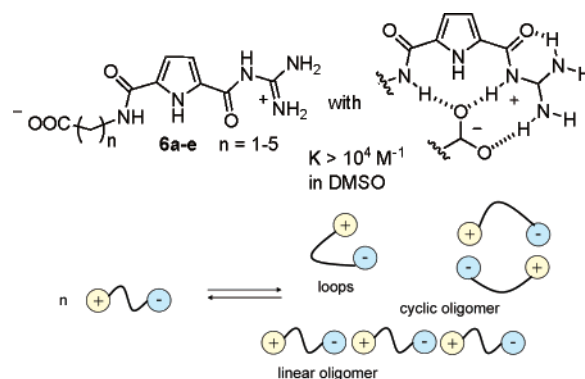
(1) (a) Lehn, J.-M. *Supramolecular Chemistry: Concepts and Perspectives*; VCH: Weinheim, 1995; (b) Bowden, N. B.; Weck, M.; Choi, I. S.; Whitesides, G. M. *Acc. Chem. Res.* **2001**, *34*, 231–238; (c) Lehn, J.-M. *Proc. Natl. Acad. Sci. U.S.A.* **2002**, *99*, 4763–4768; (d) Whitesides, G. M.; Boncheva, M. *Proc. Natl. Acad. Sci. U.S.A.* **2002**, *99*, 4769–4774; (e) Hoeben, F. J. M.; Jonkheijm, P.; Meijer, E. W.; Schenning A. H. P. J. *Chem. Rev.* **2005**, *105*, 1491–1546.

supramolecular oligomerization has so far often relied on the additional help of strong metal–ligand or extensive hydrophobic interactions.⁵ In this context, we currently investigate how ionic interactions can be used to enhance the strength of H-bonded assemblies.^{6,7} We have now synthesized a new class of flexible zwitterions **6a–e**, in which a carboxylate is linked via an alkyl chain with variable length (one to five methylene groups) to a guanidiniocarbonylpyrrole cation, one of the most efficient carboxylate binding motifs known.⁸ Depending on the length and therefore flexibility of the alkyl spacer these zwitterions in principle can either fold intramolecularly or form linear or cyclic oligomers (Scheme 1).^{9,10}

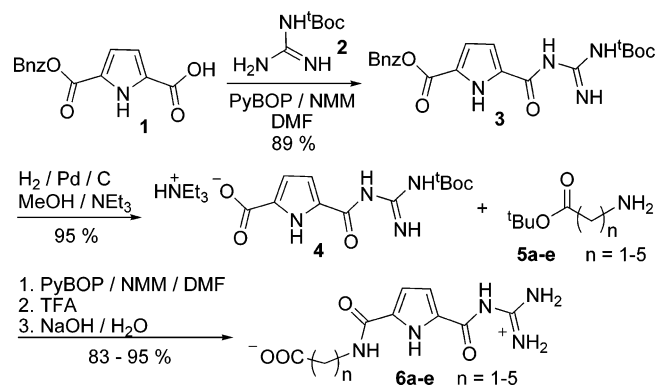
Results and Discussion

Synthesis of the Zwitterions. The zwitterions **6a–e** were synthesized according to Scheme 2: The monoprotected pyrrole bis-carboxylic acid **1** was coupled with mono-Boc-protected guanidine **2**¹¹ using PyBOP as the coupling reagent to yield the acylguanidine derivative **3**. Because of the reduced reactivity of pyrrolecarboxylic acids no other coupling reagent (such as DCC or EDIC) nor the more readily available diprotected

SCHEME 1. Self-Assembly of Flexible Zwitterions Such as **6** Can in Principle Lead to Various Aggregates Depending on the Length and Flexibility of the Spacer in between the Two Opposite Charges



SCHEME 2. Synthesis of Flexible Zwitterions **6a–e** by Coupling of the *tert*-Butyl Esters **5a–e** with the Boc-Protected Guanidiniocarbonylpyrrole **4**



(2) (a) Ciferri, A. *Supramolecular Polymers*; Taylor & Francis: New York, 2005; (b) Brunsvelde, L.; Folmer, B. J. B.; Meijer, E. W.; Sijbesma R. P. *Chem. Rev.* **2001**, *101*, 4071–4097; (c) Schmuck C.; Wienand, W. *Angew. Chem., Int. Ed.* **2001**, *40*, 4363–4369; (d) Sherrington, D. C.; Taskinen K. A. *Chem. Soc. Rev.* **2001**, *30*, 83–93.

(3) (a) Prins, L. J.; Reinhoudt, D. N.; Timmermann, P. *Angew. Chem., Int. Ed.* **2001**, *40*, 2382–2426; (b) Zimmermann, S. C.; Corbin P. S. *Struct. Bond.* **2000**, *63*–93; (c) Rebek, J., Jr. *Acc. Chem. Res.* **1999**, *32*, 278–286; (d) Whitesides, G. M.; Simanek, E. E.; Mathias, J. P.; Seto, C. T.; Chin, D. N.; Mammen, M.; Gordon, D. M. *Acc. Chem. Res.* **1995**, *28*, 37–44.

(4) Two recent reviews on the challenge of bringing supramolecular chemistry into water can be found in (a) Oshovsky, G. V.; Reinhoudt, D. N.; Verboom, W. *Angew. Chem., Int. Ed.* **2007**, *46*, 2366–2393; (b) Kubik, S.; Reyheller, C.; Stuewe, S. *J. Incl. Phenom. Macrocycl. Chem.* **2005**, *52*, 137–187.

(5) For a recent review on metallo-supramolecular polymers, see Gohy, J.-F.; Lohmeijer, B. G. G.; Schubert, U. S. *Chem. Eur. J.* **2003**, *9*, 3472–3479.

(6) For previous work from our group on rigid as well as bis-zwitterions, see (a) Schmuck, C.; Wienand, W. *J. Am. Chem. Soc.* **2003**, *125*, 452–459; (b) Schmuck, C. *Tetrahedron* **2001**, *57*, 3063–3067; (c) Schmuck, C.; Rehm, T.; Klein, K.; Gröhn, F. *Angew. Chem., Int. Ed.* **2007**, *46*, 1693–1697; (d) Schmuck, C.; Rehm, T.; Gröhn, F.; Klein, K.; Reinhold, F. *J. Am. Chem. Soc.* **2006**, *128*, 1431–1431.

(7) In principle, ion-pair reinforced hydrogen bonds (ionic or charged H-bonds) are significantly stronger than neutral H-bonds: (a) M. Nautner *Chem. Rev.* **2005**, *105*, 213–284; (b) Cooke, G.; Rotello, V. M. *Chem. Soc. Rev.* **2002**, *31*, 275–286. For some selected examples, see (c) Kienhoefer, A.; Kast, P.; Hilvert, D. *J. Am. Chem. Soc.* **2003**, *125*, 3206–3207; (d) Chapman, R. G.; Sherman, J. C. *J. Am. Chem. Soc.* **1998**, *120*, 9818–9826; (e) Mascal, M.; Fallon, P. S.; Batsanov, A. S.; Heywood, B. R.; Champ, S.; Colclough, M. *J. Chem. Soc., Chem. Commun.* **1995**, *8*, 805–806.

(8) For reviews on anion recognition including guanidinium cations, see (a) Schug, K. A.; Lindner, W. *Chem. Rev.* **2005**, *105*, 67–113; (b) Fitzmaurice, R. J.; Kyne, G. M.; Douheret, D.; Kilburn, J. D. *J. Chem. Soc., Perkin Trans. 1* **2002**, 841–846; (c) Best, D. M.; Tobey, S. L.; Ansllyn, E. V. *Coord. Chem. Rev.* **2003**, *240*, 3–15; (d) Schmidtchen, F. B.; Berger, M. *Chem. Rev.* **1997**, *97*, 1609–1646.

(9) For general reviews on foldamers, see (a) Hill, D. J.; Mio, M. J.; Prince, R. B.; Hughes, T. S.; Moore, J. S. *Chem. Rev.* **2001**, *101*, 3893–4012; (b) Cubberley, M. S.; Iverson, B. L. *Curr. Opin. Chem. Biol.* **2001**, *5*, 650–653.

(10) For some specific examples how folding of flexible molecules affects their properties see: a) Rotger, C.; Neues Pina, M.; Vega, M.; Ballester, P.; Deyà, P. M.; Costa, A. *Angew. Chem., Int. Ed.* **2006**, *45*, 6844; b) Archer, E. A.; Krische, M. J. *J. Am. Chem. Soc.* **2002**, *124*, 5074–5083; c) Schmuck, C. *J. Org. Chem.* **2000**, *65*, 2432–2437; d) Szafran, M.; Dega-Szafran, Z.; Katrusiak, A.; Buczak, G.; Glowiak, T.; Stikowski, J.; Stefaniak, L. *J. Org. Chem.* **1998**, *63*, 2898–2908.

(11) Zapf, C. W.; Creighton, C. J.; Tomioka, M.; Goodman, M. *Org. Lett.* **2001**, *3*, 1133–1136.

guanidines, otherwise often used for guanidylations,¹² worked in this case. After removal of the benzyl ester in **3** via hydrogenation, the resulting free carboxylic acid group in **4** was coupled with the *tert*-butylester of the ω -amino acid **5a–e** ($n = 1–5$).¹³ Subsequent deprotection of the Boc group and the *tert*-butyl ester with trifluoroacetic acid and pH adjustment with aqueous sodium hydroxide solution to a value of 5 to 6 led to the zwitterionic compounds **6**. The zwitterionic protonation state of **6** was confirmed in the NMR spectra.

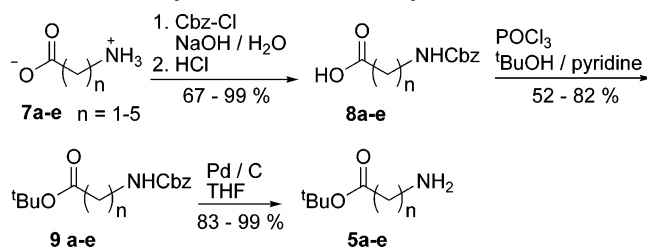
The *tert*-butyl esters of the ω -amino acid **5a–e** needed for this synthesis were synthesized according to a literature procedure shown in Scheme 3 starting from the free ω -amino acids **7**.¹⁴ After protecting the primary amino group in **7** as a benzyl carbamate, the carboxylic acid group was transformed into the *tert*-butyl esters by reaction with phosphoryl chloride and *tert*-butanol alcohol in pyridine.¹³ Deprotection of the amino group via hydrogenation with Pd on activated charcoal then provided the desired *tert*-butyl esters **5a–e**.

A second, shorter synthetic route to these zwitterions was also developed (Scheme 4). For example, for the synthesis of **6d** ($n = 4$), first 6-aminovaleric acid **10** was stirred with

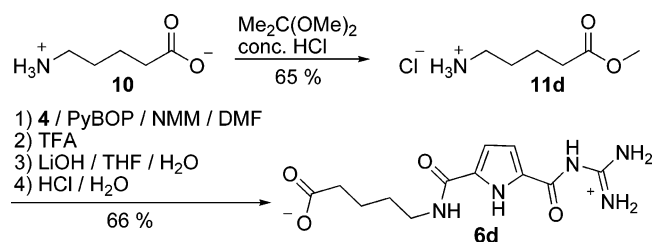
(12) (a) Feichtinger, K.; Zapf, C.; Sings, H. L.; Goodman, M. *J. Org. Chem.* **1998**, *63*, 3804–3805; (b) Powell, D. A.; Ramsden, P. D.; Batey, R. B. *J. Org. Chem.* **2003**, *68*, 2300–2309.

(13) Ruijtenbeek, R.; Kruijtzter, J. A. W.; van de Wiel, W.; Fischer, M. J. E.; Flück, M.; Redegeld, F. A. M.; Liskamp, R. M. J.; Nijkamp, F. P. *Chem. BioChem.* **2001**, *2*, 171–179.

(14) Moyer, M. P.; Feldman, P. L.; Rapoport, H. *J. Org. Chem.* **1985**, *50*, 5223–5230.

SCHEME 3. Synthesis of the *tert*-Butyl Esters 5a–e

SCHEME 4. Alternative Synthesis for the Methyl Ester 11d and Zwitterion 6d



concentrated hydrochloric acid and 2,2-dimethoxypropane to give the methyl ester **11d**.¹⁵ After coupling of **11d** with **4** using PyBOP, subsequent deprotection first with trifluoroacetic acid and then with lithium hydroxide gave the free zwitterion **6d**. Although this route leads to the orthogonally bis-protected zwitterion as an intermediate and therefore requires a two-step deprotection, the main advantage is the easier access to the amino ester **11** compared to the route described in Scheme 3.

Self-Association of Zwitterion 6a (n = 1). We first studied the self-association of the smallest zwitterion **6a** (*n* = 1) using NMR dilution experiments in DMSO-*d*₆.¹⁶ The solubility of zwitterion **6a** is limited to concentrations <25 mM already hinting to the formation of some kind of larger aggregates in solution. The concentration dependent shifts of the various NHs clearly indicate an *intermolecular* interaction of the carboxylate anion of one molecule with the guanidiniocarbonylpyrrole cation of another. For example, the signal for the guanidinium amide NH shifts from $\delta \leq 10.6$ in a highly diluted solution (0.05 mM) to a limiting $\delta \approx 11.25$ already at a concentration >10 mM (Figure 1). Hence, a rather strong intermolecular self-aggregation for **6a** (*n* = 1) occurs even in DMSO.

The dilution data cannot be fitted using a simple 1:1-dimerization model.¹⁷ Hence, more complex self-association equilibria with formation of higher oligomers must be present in solution. On the basis of statistical arguments at lower concentrations, most likely cyclic oligomers prevail whereas at higher concentrations linear oligomers should be present. This is a general finding for supramolecular oligomerization. Below a certain critical concentration only small rings exist and above which a so-called ring-to-chain transition takes place.^{18,19} At this point the number of rings has reached a certain saturation level and only slowly increases further with increasing concen-

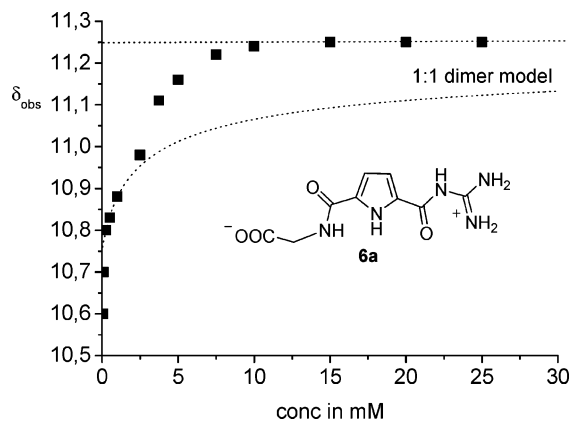


FIGURE 1. Shift change of the guanidinium amide NH of **6a** obtained from a NMR dilution experiment in DMSO-*d*₆. The dotted line represents the expected shift changes for a 1:1-dimerization leading to the same limiting shift value.

tration because of the formation of larger rings. However, the amount of linear oligomers significantly increases, finally exceeding that for rings.¹⁹

From the chemical shift of the free monomer ($\delta_{\text{free}} \leq 10.60$), the limiting shift of the oligomer ($\delta_{\text{oligo}} = 11.25$), and the observed chemical shift at 5 mM ($\delta_{\text{obs}} = 11.16$), one can estimate that the degree of polymerization (DP) at this concentration is already DP ≈ 8 using the following equation (assuming a stepwise, noncooperative linear oligomerization with constant interaction energies for each step):^{2a,18b}

$$DP = \frac{1}{1-p} \text{ with } p = \frac{\delta_{\text{obs}} - \delta_{\text{free}}}{\delta_{\text{oligo}} - \delta_{\text{free}}}$$

This strong tendency of **6a** to self-associate is also supported by ESI-MS experiments from DMSO/MeOH solution. In addition to the monomer, even at very low concentrations (≤ 1 mM) signals for oligomers such as dimers and trimers can be observed (Figure 2). The formation of even larger oligomers at higher concentrations as suggested by the NMR dilution studies is furthermore supported by dynamic light scattering experiments, which indicate the formation of large aggregates with up to a size of 100 nm in solution. Unfortunately, because of solubility problems and beginning precipitation at higher concentrations a detailed quantitative analysis of the scattering data was not possible.

Self-Association of Zwitterions 6b–e (n = 2–5). We then studied the self-association of the more flexible zwitterions **6b–e** (*n* = 2–5) again using NMR dilution experiments. Compared to **6a** the other zwitterions are much more soluble in DMSO. Concentrations of 100 mM can easily be achieved. All zwitterions again show a significant downfield shift of the guanidinium amide NH with increasing concentration (Figure 3). This proves that an *intermolecular* self-association takes place. However, much higher concentrations are needed to reach the limiting shifts of the various aggregates in the NMR dilution studies

(15) Oelofson, W.; Li, C. H. *J. Org. Chem.* **1968**, *33*, 1581–1583.

(16) (a) Wilcox, C. S. in *Frontiers in Supramolecular Chemistry and Photochemistry*; Schneider, H. J.; Dürr, H., Eds.; VCH: Weinheim, 1990; (b) Connors, K. A. *Binding Constants*; Wiley: New York, 1987.

(17) (a) Bangert, B. W.; Chan, S. I. *J. Am. Chem. Soc.* **1969**, *91*, 3910–3921; (b) Davis, J. C. Jr.; Deb, K. K. *Adv. Magn. Reson.* **1970**, *4*, 201–270.

(18) For an experimental demonstration of this ring-to-chain transition, see (a) Söntjens, S. H. M.; Sijbesma, R. P.; van Genderen, M. H. P.; Meijer, E. W. *Macromolecules* **2001**, *34*, 3815–3818; (b) Yamaguchi, N.; Nagvekar, D. S.; Gibson, H. W. *Angew. Chem., Int. Ed.* **1998**, *37*, 2361–2364.

(19) For a thorough theoretical treatment of ring-chain equilibria in self-assembly and related phenomena, see (a) Chen, C.-C.; Dormidontova, E. E. *Macromolecules* **2004**, *37*, 3905–3917; (b) Ercolani, G. *J. Phys. Chem. B* **2003**, *107*, 5052–5057; (c) Ercolani, G. *J. Am. Chem. Soc.* **2003**, *125*, 16097–16103; (d) Galli, C.; Mandolini, L. *Eur. J. Org. Chem.* **2000**, 3117–3125; (e) Ercolani, G.; Mandolini, L.; Mencarelli, P.; Roelens, S. *J. Am. Chem. Soc.* **1993**, *115*, 3901–3908.

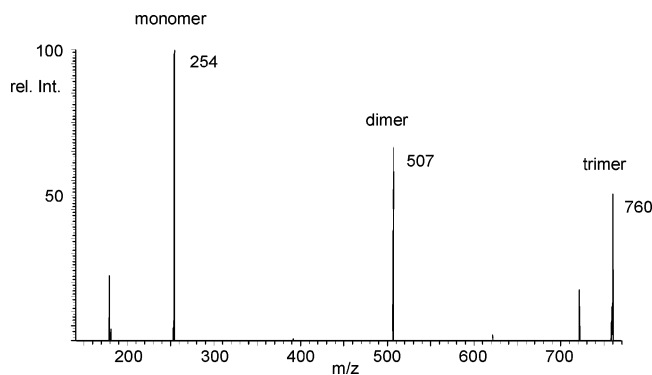


FIGURE 2. ESI MS spectrum of **6a**. In addition to the M^+ signal at $m/z = 254$ the intensive signals at $m/z = 507$ and 760 indicate the formation of supramolecular oligomers in solution (1 mM solution in DMSO).

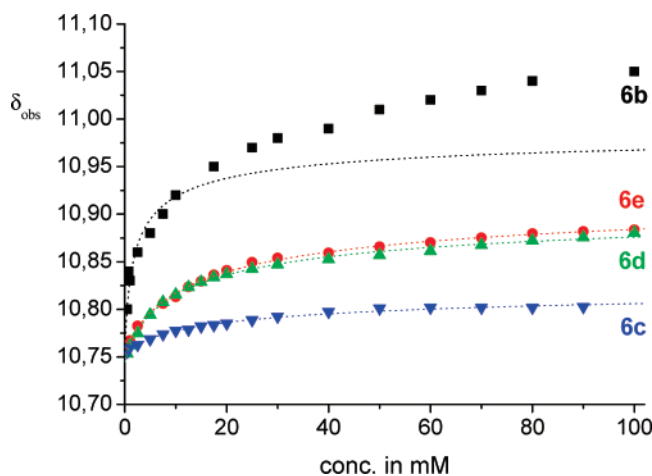


FIGURE 3. NMR dilution data of the guanidinium amide NH of **6b–e** (in $DMSO-d_6$). The dotted lines represent the curve fittings according to a 1:1-dimerization model.

(e.g., >80 mM for **6b**). Therefore, the self-association of the more flexible zwitterions **6b–e** is obviously significantly weaker than for **6a**.

The most striking difference between these four zwitterions is the different limiting shift values which are observed at higher concentrations. Whereas **6b** approaches a value similar to zwitterion **6a** ($\delta \approx 11.16$ versus 11.24 for **6a**, respectively), the limiting value for the longer zwitterions **6c–e** are significantly smaller ($\delta = 10.83$ for **6c** and $\delta = 10.93$ for **6d** and **6e**, respectively). This suggests that the structures of the self-assembled aggregates are different for all zwitterions. In contrast to zwitterion **6a**, the shift changes for zwitterions **6c–e** ($n = 3–5$) can be perfectly well fitted over the whole concentration range to a 1:1-dimerization according to the following equation:^{16,17}

$$\delta_{\text{obs}} = \delta_{\text{free}} + \frac{1 + 4K_{\text{ass}}C - \sqrt{1 + 8K_{\text{ass}}C}}{4K_{\text{ass}}C} \times (\delta_{\text{oligo}} - \delta_{\text{free}})$$

The calculated association constants for dimer formation are $K \approx 30–50 \text{ M}^{-1}$ for **6c–e** with no significant differences between these three zwitterions. The degree of polymerization at 50 mM is estimated to be $DP \approx 2$ for **6c–e** (in agreement with the good fit of the NMR data to a 1:1-dimer model over the whole concentration range, Figure 3). Of course, this

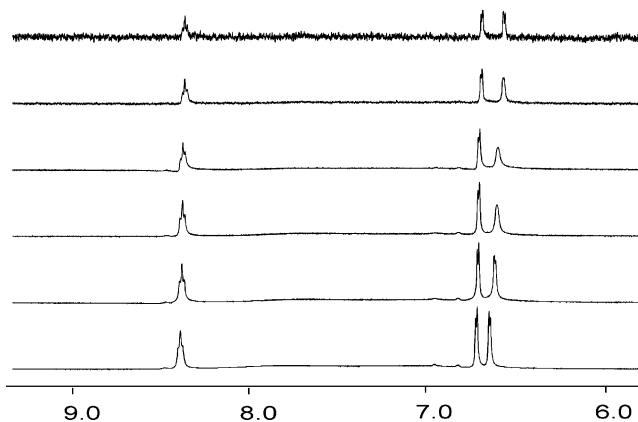


FIGURE 4. Shift change of the guanidinium amide NH of **6b** obtained from a NMR dilution experiment in $DMSO-d_6$. For example, the pyrrole CH signal at $\delta = 6.7$ with increasing concentration of the solution first broadens and then sharpens again (concentrations from top to bottom: 0.1 mM to 80 mM).

discussion is based on and hence limited to aggregations due to the directed ion-pair formation which causes shift-changes in the NMR. Any further, NMR-silent unspecific aggregation cannot be completely excluded. At higher concentrations additional larger aggregates due to unspecific interactions between the dimers might therefore also form to some extent. However, at least in the concentration range studied ESI-MS-experiments also do not give any hints for such further aggregation (*vide infra*).

For zwitterion **6b** ($n = 2$) especially at higher concentrations a significant deviation from the 1:1-dimerization model is observed, indicating again the formation of even larger aggregates in combination with simple dimerization. This is also in agreement with the NMR dilution data of **6b**, as the initially sharp signals of the monomer first become rather broad with increasing concentration before sharpening again at even higher concentrations (e.g., the signal at $\delta \approx 6.7$ in Figure 4). This could hint first to the formation of cyclic oligomers which are still rather flexible, giving rise to broader signals in the NMR. With increasing concentration these cyclic oligomers then rearrange most likely to linear oligomers with a more defined structure and hence sharper NMR signals.

In ESI-MS experiments intense signals for dimers of **6b** are observed (already from diluted DMSO solutions) as well as smaller signals for larger oligomers (trimers and tetramers). However, the intensity of the signals for the larger aggregates relative to the monomer is significantly smaller than in the case of **6a**. For **6c** the predominant signal in diluted solutions is the monomer and only a small signal for the dimer is seen (Figure 5). However, when the concentration of the solution is increased, the signal for the dimer increases significantly in relative intensity. For example, in the ESI-MS spectrum of **6c** obtained from a 10 mM solution the ratio of dimer to monomer is ca. 1:10 whereas it is already 1:3 at 100 mM and nearly 1:1 in a 150 mM solution. But no signals of significant intensity for any larger aggregates are observed.

Data Interpretation. From the above-mentioned experiments, one can deduce that all zwitterions self-assemble in DMSO, but the stability of the aggregates and hence most likely also their size significantly changes in the order **6a** \gg **6b** $>$ **6c** \approx **6d** \approx **6e**. In principle, the stability decreases with increasing

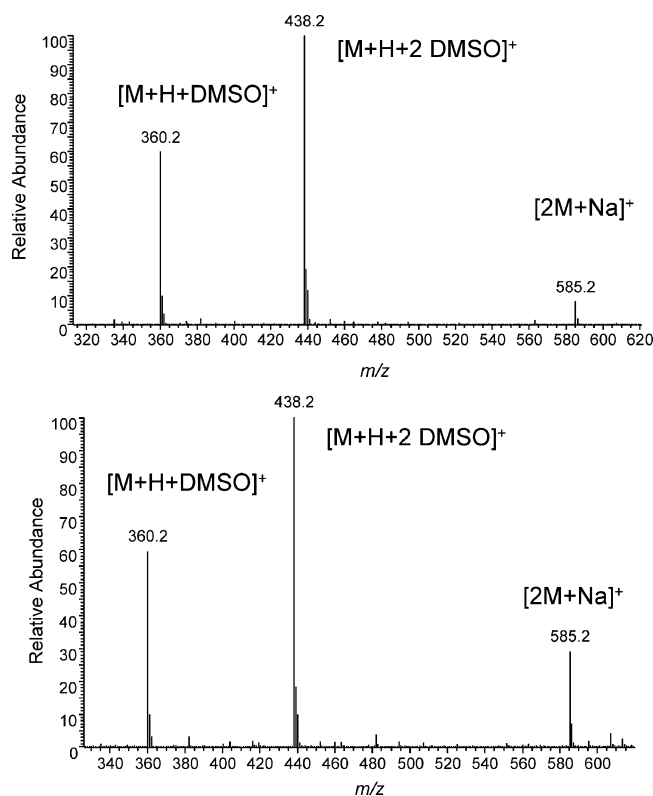
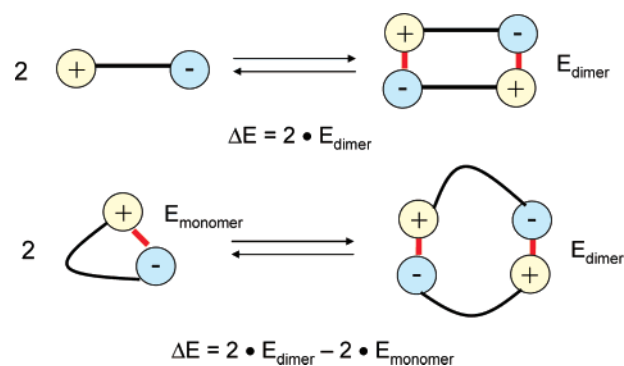


FIGURE 5. ESI-MS spectra of **6c** obtained from a DMSO solutions with a concentration of 10 mM (top) and 100 mM (bottom). The increasing intensity of the dimer signal at $m/z = 585$ relative to the signals for the monomers ($m/z = 438$) indicates the formation of self-assembled dimers with increasing concentration.

length of the linker. This is generally found for supramolecular oligomerization of flexible monomers.^{19a} However, there is a pronounced difference in aggregation behavior between **6b** and **6c**. From **6c** onward, all longer zwitterions behave in a very similar manner. The stability of the dimers ($K \leq 50 \text{ M}^{-1}$) formed by zwitterions **6c–e** is several orders of magnitude weaker than expected for the interaction between a carboxylate and a guanidiniocarbonylpyrrole cation, which has an association constant of $K \approx 10^5 \text{ M}^{-1}$ in DMSO.²⁰ For the smaller zwitterion **6b** the stability increases as seen by the more pronounced presence of larger aggregates in solution (e.g., in the ESI-MS). The smallest zwitterion **6a** forms even more stable aggregates than **6b** even though their stability cannot be determined directly from the NMR dilution data because of the complex mixture of different coexisting oligomers.

Why is the intermolecular ion pair formed by the longer zwitterions less stable than expected for the interaction of a carboxylate with a guanidiniocarbonylpyrrole cation? The reason is that for these flexible zwitterions already in the monomer a significant *intramolecular* ion pairing is possible between the carboxylate and the cationic guanidiniocarbonylpyrrole group. Hence, the dimerization energy reflects only the difference between this *intramolecular* ion pairing within the monomer and the *intermolecular* ion pairing within the dimers (Scheme 5). This difference is of course much smaller than the interaction energy for two opposite charges or a rigid zwitterion without the possibility of any intramolecular charge compensation. We

SCHEME 5. Intramolecular Ion Pairings within Flexible Zwitterions (bottom) Reduce the Stability of the Dimer (or any other larger oligomer) Compared to Rigid Zwitterions (top)



could recently show that for a completely rigid guanidiniocarbonylpyrrole zwitterion, which has a dimerization energy of $K > 10^{10} \text{ M}^{-1}$ in DMSO,^{6a} this lack of intramolecular charge compensation is one of the dominant factors responsible for the extraordinary large dimer stability.²¹ Vice versa, any intramolecular ion pairing will stabilize the monomer relative to the dimer (or any other oligomer) and hence significantly reduce the dimerization energy. This explains why flexible zwitterions interact much less efficiently with each other than rigid ones.

Within this series of flexible zwitterions **6a–e**, the length of the linker determines the efficiency of the intramolecular ion pairing. For **6a** ($n = 1$), an ion pairing within the monomer is hardly possible because of geometric reasons (the linker is too short), resulting in a significantly stronger self-association of **6a** compared to the other four zwitterions and therefore the formation of much larger aggregates. For **6b**, some charge stabilization might be possible within the monomer but the linker is still too short, allowing only a limited stabilization of the monomer. From **6c** onward, the linker is then long enough to allow significant ion pairing already within the monomer, dramatically increasing its stability and hence destabilizing larger aggregates. The energy-minimized structure of the monomer **6b** and **6c** as obtained from a molecular mechanics calculation (Macromodel Model V 8.0, Amber* force field, GB/SA water solvation)²² confirms the possibility for an intramolecular charge compensation in the case of **6c** but not for **6b** (Figure 6). The energy-minimized structure for **6b** is an extended conformation with the carboxylate pointing away from the guanidiniocarbonylpyrrole cation. For **6c** with the longer linker, the carboxylate folds back toward the cation, giving rise to some intramolecular ion pairing. This is also supported by the observed NMR shifts for highly diluted solutions (which predominantly contain monomeric species at least for **6c–e**): The guanidinium amide NH of zwitterions **6c–e** ($\delta \approx 10.75$) appear at lower fields than those of **6a** and **6b** ($\delta \leq 10.6$), respectively. That the critical linker length for beginning intramolecular ion pairing is between **6b** and **6c** was also confirmed by high level ab initio DFT calculations (BLYP/TZVPP-RI) on gas-phase structures of the monomers. For **6b** the most stable structure is the neutral one with an extended conformation. For **6c**, a back-folded zwitter-

(21) Schlund, S.; Schmuck, C.; Engels, B. *J. Am. Chem. Soc.* **2005**, *127*, 11115–11124.

(22) Mohamadi, F.; Richards, N. G. J.; Guida, W. C.; Liskamp, R. M. J.; Lipton, M.; Caufield, C.; Chang, G.; Hendrickson, T.; Still, W. C. *J. Comput. Chem.* **1990**, *11*, 440–467.

(20) (a) Schmuck, C. *Chem. Eur. J.* **2000**, *6*, 709–718; (b) Schmuck, C. *Eur. J. Org. Chem.* **1999**, 2397–2403.

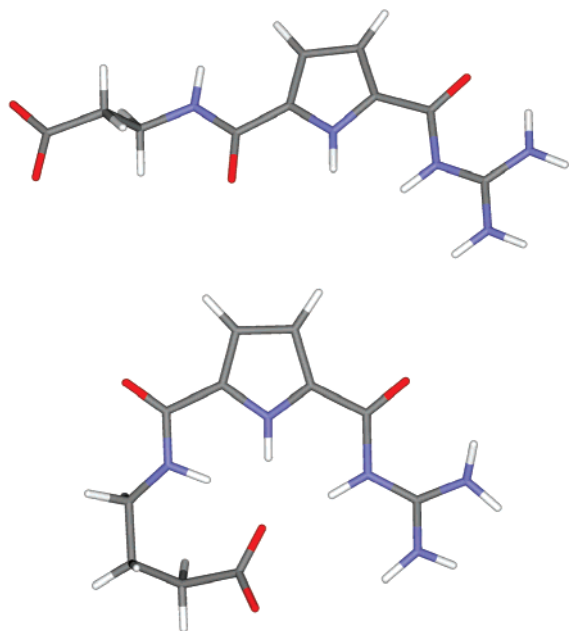


FIGURE 6. Energy-minimized structure of zwitterions **6b** (top) and **6c** (bottom) obtained from molecular mechanics calculations. The more flexible C3-linker in **6c** allows an intramolecular ion pairing between the carboxylate and the guanidiniocarbonylpyrrole cation which is not possible in **6b**.

ionic structure is energetically more favorable (similar to the MM calculations in solution shown in Figure 6).

The same observation was recently made by us in gas phase in ESI-FT-ICR MS experiments.²³ The formation of zwitterionic structures in the gas phase is normally not favorable if no significant intramolecular charge stabilization is possible. For example, amino acids, even though zwitterionic in solution, are neutral in the gas phase.²⁴ The same holds for zwitterion **6a** and **6b** which both are also neutral in the gas phase. From **6c** onward, however, even in the gas phase the zwitterionic form is more stable due to a significant intramolecular charge stabilization. Therefore, the observed differences in the self-association behavior of the five flexible zwitterions presented here can be explained based on the length of the linker and the differing degree of intramolecular charge stabilization within the monomer. The extent of intramolecular charge compensation is, however, not linearly dependent on the length of the linker. There is a critical minimum length which in this specific case requires a linker with at least three carbons.

Conclusions

In conclusion, we have shown here how the individual self-assembling properties of a series of related flexible zwitterions depend on the relative extent of intra- versus intermolecular ion pairing. Increasing stabilization of the monomer due to

intramolecular ion pairing prevents efficient self-assembly and hence the formation of larger aggregates. Only zwitterion **6a** (and to a lesser extent also **6b**), in which intramolecular ion pairing is not possible, forms large aggregates. The critical linker length which allows significant intramolecular ion pairing in this series is three carbons. Therefore, from **6c** onward, only weak intermolecular self-association is observed. Consequently, for the design of efficient building blocks, e.g., for supramolecular polymers, not only the strength of the interaction between the self-complementary end groups per se is important but also the rigidity or flexibility of the building block and any monomer stabilization resulting thereof.

Experimental Section

All solvents were dried and distilled under nitrogen before use. The chemical shifts are reported relative to the solvent.

Benzyl 5-*N*-Boc-Guanidiniocarbonyl-1*H*-pyrrole-2-carboxylate (3). A mixture of the benzyl ester **1** (1.0 g, 4.07 mmol, 1 equiv), PyBOP (2.33 g, 4.48 mmol, 1.1 equiv), and *N*-methylmorpholine (1 mL, 9.09 mmol) was stirred in DMF (20 mL) at room temperature for 30 min. ¹Boc-guanidine **2** (1.30 g, 8.14 mmol, 2 equiv) was added, and the resulting solution was stirred overnight. The red solution was slowly poured into vigorously stirred water (60 mL). A slightly yellow solid precipitated and was extracted with diethyl ether (3 × 50 mL). The organic phase was dried (MgSO₄), and upon evaporation of the solvent under reduced pressure a white solid precipitated. The resulting suspension was kept at 0 °C for some hours to allow full crystallization. After that the white solid was filtered and washed with cold diethyl ether and dried *in vacuo*. The remaining part of the product in solution was purified by column chromatography (SiO₂, hexane/ethyl acetate = 3/2 + 1 mL triethylamine per 100 mL), yielding a colorless crystalline powder. (in summa 1.35 g, 89%). mp: 88 °C; *R*_f = 0.51 (SiO₂, hexane/ethyl acetate = 3/2 + 1 mL triethylamine per 100 mL eluent); ¹H NMR (400 MHz, DMSO-*d*₆) δ = 1.45 (s, 9H, CH₃), 5.30 (s, 2H, CH₂), 6.83 (m, 2H, CH), 7.30–7.46 (m, 5H, CH), 8.56 (br s, 1H, NH), 9.30 (br s, 1H, NH), 10.73 (br s, 1H, NH), 11.61 (br s, 1H, NH); ¹³C NMR (100 MHz, DMSO-*d*₆) δ = 27.9 (CH₃), 65.7 (CH₂), 116.0 (CH), 128.1 (CH), 128.2 (CH), 128.6 (CH), 136.4 (Cq); 158.5 (Cq), 160.0 (Cq); FT-IR $\tilde{\nu}$ (KBr-pellet) [cm⁻¹] = 3393 [m], 3256 [m], 2360 [s], 2340 [m], 1719 [s], 1717 [s], 1635 [s], 1540 [s], 1286 [s], 1149 [s], 842 [w]; HR-MS (ESI pos.) *m/z* = 409.149 (calculated for M + Na⁺: 409.146). [s], 1149 [s], 842 [w]; HR-MS (ESI pos.) *m/z* = 409.149 (calculated for M + Na⁺: 409.146).

Triethylammonium 5-*N*-Boc-Guanidiniocarbonyl-1*H*-pyrrole-2-carboxylate (4). A mixture of the benzyl ester **3** (1.00 g, 2.68 mmol) and 10% Pd/C (100 mg) in methanol (20 mL) and triethylamine (1 mL) was vigorously stirred at 40 °C for 5 h under hydrogen atmosphere. The resulting solution was filtered through a G4-frit with a Celite pad, which was washed several times with methanol/triethylamine. The solvent was evaporated under reduced pressure. After adding water (10 mL) to the resulting oil, the solution was lyophilized yielding the product as a white solid (1.01 g, 95%). mp: >300 °C; ¹H NMR (400 MHz, DMSO-*d*₆) δ = 1.09 (t, 9H, *J* = 7.2, CH₃), 1.45 (s, 9H, CH₃), 2.82 (q, 6H, *J* = 7.2, CH₂), 6.51 (d, 1H, *J* = 3.8, CH), 6.77 (s, 1H, *J* = 3.8, CH), 8.58 (br s, 1H, NH), 9.33 (br s, 1H, NH), 10.91 (br s, 2H, NH), 11.67 (br s, 1H, NH); ¹³C NMR (100 MHz, DMSO-*d*₆) δ = 9.57 (CH₃), 27.7 (CH₃), 45.2 (CH₃), 80.4 (Cq), 112.5 (CH), 114.0 (CH), 129.4 (Cq), 132.0 (Cq), 158.4 (Cq), 163.4 (Cq), 167.5 (Cq), 170.0 (Cq); FT-IR $\tilde{\nu}$ (KBr-pellet) [cm⁻¹] = 3393 [m], 2958 [w], 1650 [s], 1542 [s], 1319 [s]; HR-MS (ESI neg.) *m/z* = 295.1046 (calculated for M - HNEt₃⁺: 295.1042).

General Procedure for the Synthesis of the *N*-Cbz-Protected Amino Acids **8a–e.** A mixture of the corresponding amino acid (1 equiv) in a 2 N aqueous sodium hydroxide solution (17 mL)

(23) Schäfer, M.; Schmuck, C.; Geiger, L.; Chalmers, M. J.; Hendrickson, C. L.; Marshall, A. G. *Int. J. Mass Spectrom.* **2004**, *237*, 33–45.

(24) In the absence of solvent molecules or metal ions, which can stabilize charges, amino acids are neutral in the gas phase (for a recent experimental work, see Blanco, S.; Lesarri, A.; Lopez, J. C.; Alonso, J. L. *J. Am. Chem. Soc.* **2004**, *126*, 11675–11683). Only for arginine does the zwitterionic form come energetically close that of the neutral form because of an internal ion pairing, but it is still less stable (ΔE about +5 kJ/mol): see e.g. (a) Julian, R. R.; Hodyss, R.; Beauchamp, J. L. *J. Am. Chem. Soc.* **2001**, *123*, 3577–3583; (b) Chapo, C. J.; Paul, J. B.; Provencal, R. A.; Roth, K.; Saykally, R. J. *J. Am. Chem. Soc.* **1998**, *120*, 12956–12957.

was cooled in an ice bath to 0 °C. Under vigorous stirring benzyl chloroformate (1.1 equiv) and a 2 N aqueous sodium hydroxide solution (19 mL) were simultaneously added within 2 min. The mixture was stirred for 20 min at room temperature and extracted with diethyl ether (4 × 40 mL). The aqueous layer was separated and acidified with conc hydrochloric acid to a pH of 2. The resulting emulsion was extracted with ethyl acetate (3 × 30 mL). The organic phases were combined, washed with brine, and dried with sodium sulfate. Concentration *in vacuo* gave white needles, which were dried under high vacuum.

8a. yield: 79%; mp: 119–120 °C; ¹H NMR (400 MHz, CDCl₃) δ = 3.67 (s, 2H, CH₂), 5.04 (s, 2H, CH₂), 7.35 (m, 5H, CH), 7.53 (br s, 1H, NH), 12.55 (br s, 1H, COOH); ¹³C NMR (100 MHz, CDCl₃) δ = 42.4 (CH₂), 65.7 (CH₂), 127.9 (CH), 128.0 (CH), 128.6 (CH), 137.2 (Cq), 156.7 (Cq), 171.8 (Cq); FT-IR $\tilde{\nu}$ (KBr-pellet) [cm⁻¹] = 3330 [s], 2939 [w], 2566 [w], 1729 [s], 1680 [s], 1538 [s], 1453 [w], 1433 [w], 1413 [w], 1322 [m], 1290 [m], 1253 [s], 1170 [w], 1055 [w], 980 [s], 912 [w], 792 [m], 764 [m], 731 [m], 702 [m], 599 [m], 499 [w], 428 [w].

8b. yield: 99%; mp: 103 °C; ¹H NMR (400 MHz, CDCl₃) δ = 2.56 (br s, 2H, CH₂), 3.44 (br s, 2H, CH₂), 5.08 (s, 2H, CH₂), 5.33 (br s, 1H, NH), 7.26–7.34 (m, 5H, CH), 8.51 (br s, 1H, COOH); ¹³C NMR (100 MHz, CDCl₃) δ = 34.6 (CH₂), 36.7 (CH₂), 67.3 (CH₂), 128.5 (CH), 128.6 (CH), 128.9 (CH), 136.8 (Cq), 156.8 (Cq), 171.7 (Cq); FT-IR $\tilde{\nu}$ (KBr-pellet) [cm⁻¹] = 3334 [s], 3070 [w], 2950 [w], 1685 [s], 1537 [s], 1220 [m], 730 [m], 697 [m].

8c. yield: 67%; mp: 59 °C; ¹H NMR (400 MHz, CDCl₃) δ = 1.77–1.84 (m, 2H, CH₂), 2.36 (t, 2H, J = 7.2, CH₂), 3.18–3.26 (m, 2H, CH₂), 5.00 (br s, 1H, NH), 5.08 (s, 2H, CH₂), 7.27–7.36 (m, 5H, CH), 9.86 (br s, 1H, COOH); ¹³C NMR (100 MHz, CDCl₃) δ = 24.9 (CH₂), 31.1 (CH₂), 40.2 (CH₂), 66.8 (CH₂), 128.0 (CH), 128.1 (CH), 128.5 (CH), 136.4 (Cq), 156.6 (Cq), 178.2 (Cq); FT-IR $\tilde{\nu}$ (KBr-pellet) [cm⁻¹] = 3332 [s], 3070 [w], 2933 [w], 1687 [s], 1549 [s], 1273 [s], 1208 [s], 694 [m].

8d. yield: 90%; mp: 105 °C; ¹H NMR (400 MHz, DMSO-*d*₆) δ = 1.38–1.52 (m, 4H, CH₂), 2.20 (t, 2H, J = 7.08, CH₂), 2.98 (dt, 2H, J = 6.68, J = 6.08, CH₂), 5.00 (s, 2H, CH₂), 7.23 (t, 1H, J = 5.4, NH), 7.28–7.38 (m, 5H, aryl-CH), 11.98 (br s, 1H, COOH); ¹³C NMR (100 MHz, DMSO-*d*₆) δ = 21.8 (CH₂), 28.9 (CH₂), 33.3 (CH₂), 39.9 (CH₂), 65.1 (CH₂), 127.7 (CH), 128.3 (CH), 137.3 (Cq), 156.1 (Cq), 174.3 (Cq); FT-IR $\tilde{\nu}$ (KBr-pellet) [cm⁻¹] = 3317 [s], 3055 [w], 3029 [w], 2954 [w], 2883 [w], 1686 [s], 1535 [s], 1281 [m], 1254 [s], 1210 [s], 751 [w], 697 [w].

8e. yield: 99%; mp: 56 °C; ¹H NMR (400 MHz, CDCl₃) δ = 1.35–1.42 (m, 2H, CH₂), 1.50–1.58 (m, 2H, CH₂), 1.63–1.70 (m, 2H, CH₂), 2.36 (t, 2H, J = 7.4, CH₂), 3.21 (m, 2H, CH₂), 4.87 (br s, 1H, NH), 5.13 (s, 2H, CH₂), 7.33–7.39 (m, 5H, CH), 9.36 (br s, 1H, COOH); ¹³C NMR (100 MHz, CDCl₃) δ = 24.2 (CH₂), 26.1 (CH₂), 29.5 (CH₂), 33.8 (CH₂), 40.8 (CH₂), 66.7 (CH₂), 128.0 (CH), 128.1 (CH), 128.5 (CH), 136.5 (Cq), 156.5 (Cq), 179.0 (Cq); FT-IR $\tilde{\nu}$ (KBr-pellet) [cm⁻¹] = 3344 [s], 3050 [w], 2920 [s], 2852 [s], 1685 [s], 1528 [s], 1273 [m], 1236 [s], 696 [w].

General Procedure for the Synthesis of the N-Cbz-Protected Amino Acid *tert*-Butyl Esters 9a–e. A mixture of the *N*-Cbz-protected amino acid (1 equiv), pyridine (27 mL), and *tert*-butyl alcohol (45.0 mL) was chilled to –10 °C. Under vigorous stirring phosphoryl chloride (1.1 equiv) was added, and the solution was stirred at –10 °C for 30 min. The clear, yellow mixture was stirred at r.t overnight, concentrated *in vacuo*, and diluted with water (20 mL). The mixture was extracted with ethyl acetate (3 × 50 mL), and the organic layers were combined, washed with water (3 × 55 mL), saturated aqueous sodium sulfate solution (3 × 55 mL), again water (3 × 55 mL), 2 N aqueous potassium hydrogen sulfate solution (3 × 55 mL), and brine (2 × 30 mL), and dried with sodium sulfate. The solvent was evaporated, yielding an orange oil, which was dried under high vacuum.

9a. yield: 63%; ¹H NMR (400 MHz, CDCl₃) δ = 1.45 (s, 9H, CH₃), 3.85 (s, 2H, CH₂), 5.10 (s, 2H, CH₂), 5.26 (br s, 1H, NH), 7.33 (m, 5H, CH); ¹³C NMR (100 MHz, CDCl₃) δ = 28.0 (CH₃),

43.4 (CH₂), 66.9 (CH₂), 82.2 (Cq), 128.1 (CH), 128.7 (CH), 137.4 (Cq), 156.2 (Cq), 169.0 (Cq); FT-IR $\tilde{\nu}$ (thin film, NaCl) [cm⁻¹] = 3352 [m], 3039 [w], 2979 [s], 1724 [s], 1523 [s], 1455 [m], 1367 [m], 1362 [w], 1223 [m], 1156 [s], 1054 [m], 993 [w], 848 [m], 752 [m], 699 [s].

9b. yield: 75%; ¹H NMR (400 MHz, DMSO-*d*₆) δ = 1.39 (s, 9H, CH₃), 2.40 (t, 2H, J = 6.7, CH₂), 2.70 (m, 2H, CH₂), 5.02 (s, 2H, CH₂), 5.33 (br s, 1H, NH) 7.25–7.33 (m, 5H, CH); ¹³C NMR (100 MHz, DMSO-*d*₆) δ = 27.9 (CH₃), 37.2 (CH₂), 38.7 (CH₂), 67.2 (CH₂), 79.7 (Cq), 128.5 (CH), 128.6 (CH), 128.9 (CH), 136.8 (Cq), 156.8 (Cq), 171.6 (Cq); FT-IR $\tilde{\nu}$ (thin film, NaCl) [cm⁻¹] = 3350 [m], 3070 [m], 2979 [m], 1725 [s], 1522 [s], 1367 [m], 740 [m], 699 [m].

9c. yield: 82%; ¹H NMR (400 MHz, CDCl₃) δ = 1.43 (s, 9H, CH₃), 1.75–1.82 (m, 2H, CH₂), 2.30 (t, 2H, J = 7.1, CH₂), 3.18–3.26 (m, 2H, CH₂), 4.90 (br s, 1H, NH), 5.09 (s, 2H, CH₂), 7.30–7.36 (m, 5H, CH); ¹³C NMR (100 MHz, CDCl₃) δ = 25.2 (CH₂), 28.0 (CH₃), 32.8 (CH₂), 40.5 (CH₂), 66.6 (CH₂), 80.5 (Cq), 128.0 (CH), 128.5 (CH), 136.6 (Cq), 156.4 (Cq), 172.5 (Cq); FT-IR $\tilde{\nu}$ (thin film, NaCl) [cm⁻¹] = 3350 [m], 3070 [w], 2976 [m], 1727 [s], 1537 [s], 698 [m].

9d. yield: 52%; ¹H NMR (400 MHz, DMSO-*d*₆) δ = 1.39 (s, 9H, CH₃), 1.42–1.52 (m, 4H, CH₂), 2.19 (t, 2H, J = 6.96, CH₂), 2.99 (dt, 2H, J = 6.56, J = 6.04, CH₂), 5.01 (s, 2H, benzyl-CH₂), 7.23 (t, 1H, J = 5.56, NH), 7.27–7.38 (m, 5H, aryl-CH); ¹³C NMR (100 MHz, DMSO-*d*₆) δ = 21.9 (CH₂), 27.7 (CH₃), 28.7 (CH₂), 34.4 (CH₂), 39.9 (CH₂), 65.1 (CH₂), 79.3 (Cq), 127.7 (CH), 128.3 (CH), 137.3 (Cq), 156.1 (Cq), 172.1 (Cq); FT-IR $\tilde{\nu}$ (KBr-pellet) [cm⁻¹] = 3345 [m], 3065 [w], 3039 [w], 2976 [s], 2935 [s], 2869 [m], 1725 [s], 1532 [s], 1455 [s], 1251 [s], 773 [w], 689 [w].

9e. yield: 62%; ¹H NMR (400 MHz, DMSO-*d*₆) δ = 1.20–1.28 (m, 2H, CH₂), 1.38 (s, 9H, CH₃), 1.45–1.47 (m, 2H, CH₂), 2.13–2.17 (m, 2H, CH₂), 2.34 (t, 2H, J = 7.4, CH₂), 2.96–2.97 (m, 2H, CH₂), 4.99 (s, 2H, CH₂), 7.21 (br s, 1H, NH), 7.30–7.37 (m, 5H, aryl-CH); ¹³C NMR (100 MHz, DMSO-*d*₆) δ = 24.2 (CH₂), 26.1 (CH₃), 29.5 (CH₂), 33.9 (CH₂), 40.5 (CH₂), 66.6 (CH₂), 80.5 (Cq), 128.0 (CH), 128.5 (CH), 136.6 (Cq), 156.4 (Cq), 172.5 (Cq); FT-IR $\tilde{\nu}$ (KBr-pellet) [cm⁻¹] = 3345 [m], 3034 [w], 2920 [m], 1686 [s], 1528 [s], 733 [w], 693 [w].

General Procedures for the Synthesis of the *tert*-Butyl Esters

5a–e. A mixture of the *N*-Cbz-protected amino acid *tert*-butyl ester and 10% Pd/C was stirred for 6 h in tetrahydrofuran at 40 °C under hydrogen atmosphere. The catalyst was filtered off through a Celite pad which was washed with ethyl acetate. The filtrate and washings were combined and evaporated to give the *tert*-butyl ester compound as an oil, which was dried under high vacuum and then used without further purification.

5a. yield: 95%; ¹H NMR (400 MHz, CDCl₃) δ = 1.44 (s, 9H, CH₃), 3.78 (br s, 2H, CH₂), 7.10 (br s, 2H, NH₂); ¹³C NMR (100 MHz, CDCl₃) δ = 27.1 (CH₃), 40.1 (CH₂), 82.6 (Cq), 165.9 (Cq); FT-IR $\tilde{\nu}$ (thin film, NaCl) [cm⁻¹] = 3350 [m], 2979 [w], 1741 [s], 1374 [m], 1253 [s], 1160 [s], 1038 [m], 843 [m].

5b. yield: 83%; ¹H NMR (400 MHz, DMSO-*d*₆) δ = 1.39 (s, 9H, CH₃), 2.28 (t, 2H, J = 6.7, CH₂), 2.70 (m, 2H, CH₂), 3.10 (br s, 2H, NH₂); ¹³C NMR (100 MHz, DMSO-*d*₆) δ = 27.9 (CH₃), 37.7 (CH₂), 38.7 (CH₂), 79.7 (Cq), 171.6 (Cq); FT-IR $\tilde{\nu}$ (thin film, NaCl) [cm⁻¹] = 3379 [m], 2977 [w], 1725 [s], 1367 [s], 1247 [s], 845 [m].

5c. yield: 94%; ¹H NMR (400 MHz, CDCl₃) δ = 1.39 (s, 9H, CH₃), 1.66–1.71 (m, 2H, CH₂), 1.77 (br s, 2H, NH₂), 2.22 (t, 2H, J = 7.2, CH₂), 2.69 (m, 2H, CH₂); ¹³C NMR (100 MHz, DMSO-*d*₆) δ = 28.0 (CH₃), 28.8 (CH₂), 32.9 (CH₂), 41.4 (CH₂), 80.1 (Cq), 172.8 (Cq); FT-IR $\tilde{\nu}$ (thin film, NaCl) [cm⁻¹] = 3372 [m], 2976 [m], 1728 [s], 1455 [m], 1367 [m], 1255 [m], 847 [m].

5d. yield: 99%; ¹H NMR (400 MHz, CDCl₃) δ = 1.35 (s, 9H, CH₃), 1.37–1.41 (m, 2H, CH₂), 1.47–1.55 (m, 2H, CH₂), 2.12 (t, 2H, J = 7.44, CH₂), 2.60 (m, 2H, CH₂); ¹³C NMR (100 MHz, CDCl₃) δ = 24.7 (CH₂), 26.2 (CH₂), 27.9 (CH₃), 33.2 (CH₂), 41.8

(CH₂), 79.8 (Cq), 171.9 (Cq); FT-IR $\tilde{\nu}$ (thin film, NaCl) [cm⁻¹] = 3375 [m], 2928 [w], 1723 [s], 1454 [s], 1369 [s], 848 [m].

5e: yield: 99%; ¹H NMR (400 MHz, CDCl₃) δ = 1.23–1.28 (m, 2H, CH₂), 1.35 (s, 9H, CH₃), 1.37–1.41 (m, 2H, CH₂), 1.47–1.55 (m, 2H, CH₂), 2.12 (t, 2H, *J* = 7.44, CH₂), 2.60 (t, 2H, *J* = 6.69, CH₂); ¹³C NMR (100 MHz, CDCl₃) δ = 24.7 (CH₂), 26.2 (CH₂), 27.9 (CH₃), 33.2 (CH₂), 35.4 (CH₂), 41.8 (CH₂), 79.8 (Cq), 171.9 (Cq); FT-IR $\tilde{\nu}$ (thin film, NaCl) [cm⁻¹] = 3378 [m], 2931 [w], 1729 [s], 1457 [s], 1367 [s], 848 [m].

Methyl 5-Aminopentanoate Hydrochloride (11d). A suspension of 5-aminopentanoic acid (4.00 g, 34.1 mmol, 1 equiv) in 2,2-dimethoxypropane (106.3 g, 1.02 mol, 30 equiv) was stirred vigorously while adding concentrated hydrochloric acid (17 mL). The solution was stirred for further 24 h at room temperature. After that, the dark red solution was concentrated in vacuo and the resulting brown solid was treated with diethyl ether. The precipitating solid was filtered off, washed several times with diethyl ether and recrystallized from ethanol/ethyl acetate (60 mL, v/v 95/5), providing the product as a white crystalline solid (3.71 g, 65%). mp: 142 °C; ¹H NMR (400 MHz, CDCl₃) δ = 1.73–1.86 (m, 4H, CH₂), 2.35–2.40 (m, 2H, CH₂), 2.99–3.11 (m, 2H, CH₂), 3.67 (s, 3H, CH₃), 8.23 (s, 3H, NH₃⁺); ¹³C NMR (100 MHz, CDCl₃) δ = 21.9 (CH₂), 27.1 (CH₂), 33.3 (CH₂), 39.8 (CH₂), 51.9 (CH₃), 173.8 (Cq); FT-IR $\tilde{\nu}$ (KBr-pellet) [cm⁻¹] = 3047 [m], 2948 [m], 2876 [m], 1735 [s], 1588 [m], 1566 [m], 1509 [m], 1441 [m], 1345 [m], 1271 [m], 1198 [s], 745 [w]; HR-MS (ESI pos) *m/z* = 132.10175 (calculated for M⁺: 132.1024).

General Procedure for the Synthesis of the Fully Protected Zwitterions of 6. A mixture of the Boc-protected guanidiniocarbonylpyrrole compound **4** (1 equiv), PyBOP (1 equiv), and *N*-methylmorpholine (2 mL) was stirred in DMF (25 mL) at r.t for 15 min. The amino ester (1.2 equiv) was added to the solution and then stirred for 12 h at room temperature. The resulting brown solution was hydrolyzed with water (50 mL), and the precipitate was filtered and dried in the desiccator over phosphorus pentoxide. The resulting solid was purified by column chromatography, yielding a colorless crystalline powder.

6a (fully protected): yield: 95%; *R*_f = 0.25 (SiO₂, cyclohexane/acetone = 3/2); mp: 157 °C; ¹H NMR (400 MHz, DMSO-*d*₆) δ = 1.40 (s, 9H, CH₃), 1.46 (s, 9H, CH₃), 3.88 (d, 2H, *J* = 5.8, CH₂), 6.81 (br s, 2H, CH), 8.56 (br s, 1H, NH), 8.71 (t, 1H, *J* = 5.8, NH), 9.32 (br s, 1H, NH), 10.83 (br s, 1H, NH), 11.20 (br s, 1H, NH); ¹³C NMR (100 MHz, DMSO-*d*₆) δ = 26.3 (CH₃), 27.7 (CH₃), 41.3 (CH₂), 80.7 (Cq), 112.0 (CH), 158.3 (Cq), 160.0 (Cq), 169.0 (Cq); FT-IR $\tilde{\nu}$ (KBr-pellet) [cm⁻¹] = 3401 [m], 3295 [m], 2978 [w], 2927 [w], 1722 [s], 1637 [s], 1544 [m], 1471 [m], 1369 [m], 1288 [s], 1236 [s], 1151 [s], 843 [w]; HR-MS (ESI pos) *m/z* = 432.185 (calculated for M + Na⁺: 432.1859).

6b (fully protected): yield: 85%; *R*_f = 0.43 (SiO₂, cyclohexane/acetone = 3/2); mp: 98 °C; ¹H NMR (400 MHz, DMSO-*d*₆) δ = 1.39 (s, 9H, CH₃), 1.46 (s, 9H, CH₃), 2.46 (t, 2H, *J* = 6.84 Hz, CH₂), 3.42 (dt, 2H, *J* = 5.8, *J* = 6.8, CH₂), 6.74–6.81 (m, 2H, CH), 8.40 (t, 1H, *J* = 5.4, NH), 8.56 (br s, 1H, NH), 9.31 (br s, 1H, NH), 10.83 (br s, 1H, NH), 11.24 (s, 1H, NH); ¹³C NMR (100 MHz, DMSO-*d*₆) δ = 27.7 (CH₃), 35.0 (CH₂), 40.2 (CH₂), 79.9 (Cq), 111.7 (CH), 159.6 (Cq), 170.6 (Cq); FT-IR $\tilde{\nu}$ (KBr-pellet) [cm⁻¹] = 3387 [w], 2921 [w], 1727 [m], 1634 [s], 1554 [s], 1301 [s], 1243 [s], 844 [m]; HR-MS (ESI pos) *m/z* = 446.201 (calculated for M + Na⁺: 446.2015).

6c (fully protected): yield: 83%; *R*_f = 0.57 (SiO₂, hexane/ethyl acetate = 3/2); mp: 100–103 °C; ¹H NMR (400 MHz, DMSO-*d*₆) δ = 1.33 (s, 9H, CH₃), 1.34 (s, 9H, CH₃), 1.62–1.69 (m, 2H, CH₂), 2.19 (t, 2H, *J* = 7.5, CH₂), 3.15–3.20 (m, 2H, CH₂), 6.71 (s, 1H, CH), 6.75 (s, 1H, CH), 8.25 (t, 1H, *J* = 5.5, NH), 8.50 (br s, 1H, NH), 9.25 (br s, 1H, NH), 10.78 (br s, 1H, NH), 11.22 (br s, 1H, NH); ¹³C NMR (100 MHz, DMSO-*d*₆) δ = 25.1 (CH₂), 28.1 (CH₃), 32.7 (CH₂), 38.4 (CH₂), 79.9 (Cq), 112.0 (CH), 158.8 (Cq), 160.0 (Cq), 172.3 (Cq); FT-IR $\tilde{\nu}$ (KBr-pellet) [cm⁻¹] = 3385 [m], 3320 [br. m.], 2979 [m], 1728 [s], 1556 [s], 1469 [s], 1393 [s], 1369

[m], 1300 [s], 1243 [s], 1152 [s], 1050 [w], 843.7 [m], 789 [w], 757 [w], 602 [w]; HR-MS (ESI pos) *m/z* = 460.217 (calculated for M + Na⁺: 460.2172).

6d (fully protected): yield: 83%; *R*_f = 0.62 (SiO₂, ethyl acetate/cyclohexane = 8/2); mp: 99 °C; ¹H NMR (400 MHz, DMSO-*d*₆) δ = 1.38 (s, 9H, CH₃), 1.46 (s, 9H, CH₃), 1.50–1.54 (m, 4H, CH₂), 2.22 (t, 2H, *J* = 6.9, CH₂), 3.22 (dt, 2H, *J* = 5.68, *J* = 5.84, CH₂), 6.76 (m, 2H, CH), 8.30 (t, 1H, *J* = 5.16, NH), 8.54 (br s, 1H, NH), 9.31 (br s, 1H, NH), 10.83 (br s, 1H, NH), 11.08 (br s, 1H, NH); ¹³C NMR (100 MHz, DMSO-*d*₆) δ = 22.1 (CH₂), 27.8 (CH₃), 28.5 (CH₂), 34.4 (CH₂), 79.4 (Cq), 111.6 (CH), 129.5 (Cq), 159.5 (Cq), 172.2 (Cq); FT-IR $\tilde{\nu}$ (KBr-pellet) [cm⁻¹] = 3386 [m], 3270 [m.], 2976 [m], 2932 [m], 1730 [s], 1632 [s], 1552 [s], 1467 [s], 1365 [s], 1298 [m], 1236 [s], 1151 [s], 835 [m], 786 [w], 755 [w], 601 [w]; HR-MS (ESI pos) *m/z* = 474.233 (calculated for M + Na⁺: 474.2328).

6d (fully protected, methyl ester): yield: 66%; *R*_f = 0.51 (SiO₂, ethyl acetate/cyclohexane = 8/2); mp: 73 °C; ¹H NMR (400 MHz, DMSO-*d*₆) δ = 1.46 (s, 9H, CH₃), 1.50–1.61 (m, 4H, CH₂), 2.34 (t, 2H, *J* = 7.32, CH₂), 3.23 (dt, 2H, *J* = 5.96, *J* = 6.16, CH₂), 3.58 (s, 3H, CH₃), 6.77 (s, 1H, CH), 6.80 (s, 1H, CH), 8.31 (t, 1H, *J* = 5.56, NH), 8.56 (br s, 1H, NH), 9.31 (br s, 1H, NH), 10.83 (br s, 1H, NH), 11.29 (br s, 1H, NH); ¹³C NMR (100 MHz, DMSO-*d*₆) δ = 22. (CH₂), 27.8 (CH₃), 28.6 (CH₂), 33.0 (CH₂), 38.2 (CH₂), 51.2 (CH₃), 80.9 (Cq), 111.7 (CH), 113.8 (CH), 129.6 (Cq), 158.5 (Cq), 159.6 (Cq), 173.3 (Cq); FT-IR $\tilde{\nu}$ (KBr-pellet) [cm⁻¹] = 3450 [s], 3402 [s], 3297 [s], 2977 [m], 2949 [m], 2877 [m], 1736 [s], 1630 [s], 1559 [s], 1510 [s], 1469 [s], 1371 [m], 1346 [s], 1292 [s], 1232 [s], 1045 [m], 838 [m], 785 [m], 753 [m], 597 [m]; HR-MS (ESI pos) *m/z* = 410.204 (calculated for M + H⁺: 410.2039).

6e (fully protected): yield: 90%; *R*_f = 0.57 (SiO₂, hexane/ethyl acetate = 3/2); mp: 100 °C; ¹H NMR (400 MHz, DMSO-*d*₆) δ = 1.27–1.33 (m, 2H, CH₂), 1.37 (s, 9H, CH₃), 1.46 (s, 9H, CH₃), 1.47–1.55 (m, 4H, CH₂), 2.18 (t, 2H, *J* = 7.32, CH₂), 3.21 (dt, 2H, *J* = 6.04, *J* = 6.72, CH₂), 6.75 (s, 1H, CH), 6.81 (s, 1H, CH), 8.28 (t, 1H, *J* = 5.44, NH), 8.56 (br s, 1H, NH), 9.31 (br s, 1H, NH), 10.84 (br s, 1H, NH), 11.26 (br s, 1H, NH); ¹³C NMR (100 MHz, DMSO-*d*₆) δ = 24.3 (CH₂), 25.8 (CH₂), 27.7 (CH₃), 28.8 (CH₂), 34.7 (CH₂), 38.4 (CH₂), 79.3 (Cq), 111.5 (CH), 113.5 (CH), 124.1 (Cq), 129.7 (Cq), 158.4 (Cq), 159.4 (Cq), 172.2 (Cq); FT-IR $\tilde{\nu}$ (KBr-pellet) [cm⁻¹] = 3400 [m], 3320 [m], 2980 [m], 1730 [s], 1550 [s], 1469 [s], 1393 [s], 1300 [m], 1243 [s], 1152 [s], 1050 [w], 843.7 [m], 789 [w], 760 [w], 602 [w]; HR-MS (ESI pos) *m/z* = 460.217 (calculated for M + Na⁺: 460.2172).

The fully protected zwitterions were deprotected and converted into their picrate salts according to the general procedures detailed in the Supporting Information.

6a (picrate salt): mp: 243–244 °C (decomp); ¹H NMR (400 MHz, DMSO-*d*₆) δ = 3.94 (d, 2H, *J* = 5.8, CH₂), 6.91–6.93 (m, 1H, CH), 7.03–7.05 (m, 1H, CH), 8.16 (br s, 4H, NH), 8.59 (s, 2H, CH), 8.82 (t, 1H, *J* = 5.8, NH), 10.95 (br s, 1H, NH), 12.47 (br s, 1H, NH); ¹³C NMR (100 MHz, DMSO-*d*₆) δ = 40.7 (CH₂), 112.6 (CH), 115.5 (CH), 124.3 (Cq), 125.2 (Cq), 125.7 (Cq), 132.2 (Cq), 142.0 (Cq), 155.0 (Cq), 159.4 (Cq), 159.5 (Cq), 161.0 (Cq), 171.1 (Cq); FT-IR $\tilde{\nu}$ (KBr-pellet) [cm⁻¹] = 3404 [m], 3325 [m], 3168 [m], 1703 [s], 1611 [s], 1557 [m], 1427 [w], 1365 [m], 1337 [s], 1268 [s], 1082 [w], 911 [w], 816 [w], 763 [w]; HR-MS (ESI pos) *m/z* = 254.089 (calculated for M⁺: 254.0889).

6b (picrate salt): mp: 250–251 °C (decomp); ¹H NMR (400 MHz, DMSO-*d*₆) δ = 3.43 (dt, *J* = 6.3 Hz, 2H, CH₂), 6.86–6.88 (m, 1H, CH), 7.01–7.03 (m, 1H, CH), 8.17 (br s, 4H, NH), 8.55 (t, *J* = 11.6, 1H, NH), 8.59 (s, 2H, CH), 10.95 (br s, 1H, NH), 12.43 (br s, 1H, NH); one CH₂ peak is superposed by the solvent signal; ¹³C NMR (100 MHz, DMSO-*d*₆) δ = 33.7 (CH₂), 35.1 (CH₂), 112.5 (CH), 115.4 (CH), 125.2 (CH), 125.4 (Cq), 132.6 (Cq), 141.9 (Cq), 154.8 (Cq), 159.1 (Cq), 159.4 (Cq), 160.8 (Cq), 172.8 (Cq); FT-IR $\tilde{\nu}$ (KBr-pellet) [cm⁻¹] = 3400 [m], 3325 [m], 3168 [m], 1705 [s], 1611 [s], 1557 [m], 1427 [w], 1370 [m], 1335 [s],

1268 [s], 1082 [w], 814 [w], 763 [w]; HR-MS (ESI pos) m/z = 268.105 (calculated for M^+ : 268.1046).

6c (picrate salt): mp: 248 °C (decomp); ^1H NMR (400 MHz, DMSO- d_6) δ = 1.70–1.77 (m, 2H, CH_2), 2.28 (t, 2H, J = 7.45, CH_2), 3.24–3.29 (m, 2H, CH_2), 6.87–6.88 (m, 1H, CH), 7.02–7.03 (m, 1H, CH), 8.15 (br s, 4H, NH), 8.43 (t, 1H, J = 5.43, NH), 8.58 (s, 2H, CH), 10.93 (br s, 1H, NH), 12.08 (br s, 1H, COOH), 12.34 (br s, 1H, NH); ^{13}C NMR (100 MHz, DMSO- d_6) δ = 24.5 (CH_2), 31.0 (CH_2), 38.2 (CH_2), 112.2 (CH), 115.5 (CH), 124.1 (Cq), 125.2 (CH), 132.8 (Cq), 141.9 (Cq), 154.8 (Cq), 159.1 (Cq), 159.4 (Cq), 160.8 (Cq), 174.1 (Cq); FT-IR $\tilde{\nu}$ (KBr-pellet) [cm^{-1}] = 3546 [w], 3388 [s], 3132 [m], 2924 [w], 1714 [s], 1634 [s], 1567 [s], 1476 [m], 1433 [m], 1287 [s], 1204 [m], 1080 [w], 616 [w]; HR-MS (ESI pos) m/z = 282.121 (calculated for M^+ : 282.1202).

6d (picrate salt): mp: 244 °C (decomp); ^1H NMR (400 MHz, DMSO- d_6) δ = 1.52–1.53 (m, 2H, CH_2), 2.25 (t, 2H, J = 6.96 Hz, CH_2), 3.23–3.27 (m, 2H, CH_2), 6.86–6.88 (m, 1H, CH), 7.05–7.06 (m, 1H, CH), 8.18 (br s, 4H, NH), 8.40 (t, 1H, J = 5.56, NH), 8.58 (s, 2H, CH), 10.99 (br s, 1H, NH), 12.34 (br s, 1H, NH); one CH_2 peak is superposed by the solvent signal; ^{13}C NMR (100 MHz, DMSO- d_6) δ = 22.0 (CH_2), 28.5 (CH_2), 33.3 (CH_2), 38.4 (CH_2), 112.2 (CH), 115.5 (CH), 125.1 (CH), 132.9 (Cq), 141.9 (Cq), 154.8 (Cq), 159.0 (Cq), 159.4 (Cq), 174.3 (Cq); FT-IR $\tilde{\nu}$ (KBr-pellet) [cm^{-1}] = 3354 [s], 3199 [m], 3092 [m], 2949 [w], 2874 [w], 1706 [s], 1609 [s], 1565 [s], 1477 [m], 1435 [m], 1366 [s], 1276 [s], 762 [w], 713 [w], 593 [w]; HR-MS (ESI pos) m/z = 296.136 (calculated for M^+ : 296.1358).

6e (picrate salt): mp: 250 °C (decomp); ^1H NMR (400 MHz, DMSO- d_6) δ = 1.27–1.36 (m, 2H, CH_2), 1.47–1.56 (m, 4H, CH_2), 2.20 (t, 2H, J = 7.2, CH_2), 3.21–3.26 (m, 2H, CH_2), 6.86–6.87 (m, 1H, CH), 7.01–7.02 (m, 1H, CH), 8.16 (br s, 4H, NH), 8.40 (t, 1H, J = 5.0, NH), 8.58 (s, 2H, picrate- CH), 10.93 (br s, 1H, NH), 12.34 (br s, 1H, NH); ^{13}C NMR (100 MHz, DMSO- d_6) δ = 24.2 (CH_2), 26.0 (CH_2), 28.8 (CH_2), 33.6 (CH_2), 38.6 (CH_2), 112.2 (CH), 115.5 (CH), 124.2 (Cq), 125.2 (CH), 132.9 (Cq), 141.9 (Cq), 154.8 (Cq), 159.0 (Cq), 159.4 (Cq), 160.8 (Cq), 174.4 (Cq); FT-IR $\tilde{\nu}$ (KBr-pellet) [cm^{-1}] = 3541 [w], 3388 [s], 2930 [w], 1711 [s], 1634 [s], 1570 [s], 1476 [m], 1430 [m], 1287 [s], 1200 [m], 1084 [w], 618 [w]; HR-MS (ESI pos) m/z = 310.152 (calculated for M^+ : 310.1515).

Acknowledgment. This work was supported by the DFG (SCHM 1501) and the Fonds der Chemischen Industrie (FCI). We also thank Prof. Bernd Engels and Sebastian Schlund (University of Würzburg) for the DFT calculations and helpful discussions.

Supporting Information Available: Spectral characterization (^1H and ^{13}C NMR spectra) of the fully protected compounds **6a–e** as well as their deprotected zwitterions as picrate salts. This material is available free of charge via the Internet at <http://pubs.acs.org>.

JO070641D